

Magnetoresistance in doped magnetic tunnel junctions: Effect of spin scattering and impurity-assisted transport

R. Jansen and J. S. Moodera

Francis Bitter Magnet Laboratory, Massachusetts Institute of Technology, Cambridge, Massachusetts 02139

(Received 29 November 1999)

The effects of spin-exchange scattering and impurity-assisted tunneling on the junction magnetoresistance (JMR) are investigated in magnetic tunnel junctions with artificially doped barriers. Spin scattering is observed when magnetic ions (Ni) are introduced, while for nonmagnetic dopants (Si), impurity-assisted tunneling occurs. The latter process is shown to be mainly elastic, and gives rise to an extra conductance that is unpolarized and reduces the overall JMR. In contrast, spin-exchange scattering is demonstrated to contribute inversely to the JMR, thereby decreasing it severely. The inelastic nature of spin scattering is reflected in a more pronounced temperature and voltage dependence of the JMR, as well as the junction resistance.

Ferromagnetic tunnel junctions have been studied intensely since they were shown to exhibit large tunneling magnetoresistance (JMR).^{1,2} Of interest are application potential, various intrinsic properties, but also the behavior of junctions that are modified from the conventional ferromagnet-insulator-ferromagnet structure. For example, incorporating clusters ferromagnetic one to study the interplay between spin-transport and the Coulomb blockade,³⁻⁶ yielding new phenomena such as magnetoresistance oscillations⁵ and enhancement.^{6,7} Also, it was recognized already decades ago that tunneling electrons can interact with magnetic barrier impurities. Both experimental⁸⁻¹⁰ and theoretical¹¹⁻¹³ work has focused on the resulting effects on the *total* tunnel conductance at low temperature (T) and small voltage (V), where spin-exchange scattering produces so-called zero-bias anomalies. Nonmagnetic impurities influence the tunnel conductance too, by creating states in the barrier that provide additional current paths.^{14,15} This is well-established for tunneling through amorphous barriers.^{16,17}

Impurity scattering can occur in spin-polarized transport in standard magnetic tunnel junctions, but also in tunnel-type granular alloys, magnetic oxides, and semiconductor-based systems, and will ultimately limit the magnetoresistance of structures consisting of 100% spin-polarized materials. A complete picture of spin-tunneling in these systems therefore requires detailed knowledge about impurity scattering, which has so far been based on theoretical work or indirect experiments without spin sensitivity.⁸⁻¹⁷ In this paper we employ the controlled preparation of magnetic tunnel junctions to uniquely and directly probe the effect of impurity scattering on the conductance and tunnel electron polarization. This is done using tunnel junctions “doped” with a well-defined amount of foreign atoms deposited in the form of a thin sheet of submonolayer thickness, in the middle of an Al_2O_3 tunnel barrier between two ferromagnetic electrodes. The JMR for such δ -doped junctions was measured as function of the nominal thickness t of the doping layer, as well as versus T and V . Although a variety of elements has been used,¹⁸ we report only results for Al_2O_3 doped with Si or Ni. We choose Si because it forms ions with no magnetic moment after oxidation. Impurity-assisted tunneling can then be studied

and we present direct experimental evidence that this process produces an unpolarized, elastic contribution to the conductance. In contrast, Ni-doping introduces magnetic ions into the barrier, and we indeed find strikingly different behavior, i.e., for Ni doping an inelastic term with an *inverse* JMR appears due to spin-exchange scattering.

A general expression for the tunnel conductance G of a doped barrier is given by

$$G = G_t + G^{\text{as}} + G^{\text{ex}}, \quad (1)$$

where

$$G_t = G_0 [1 + P_1 P_2 \cos(\theta)], \quad (2)$$

$$G^{\text{as}} = G_0^{\text{as}} [1 + P_1^{\text{as}} P_2^{\text{as}} \cos(\theta)], \quad (3)$$

$$G^{\text{ex}} = G_0^{\text{nsf}} [1 + P_1 P_2 \cos(\theta)] + G_0^{\text{sf}} [1 - P_1 P_2 \cos(\theta)]. \quad (4)$$

The first contribution G_t describes the process of direct, spin-conserved tunneling, in terms of the *effective* tunneling spin polarization P_1 and P_2 of electrode 1 and 2, respectively.¹⁹ The prefactor G_0 controls the total conductance, while θ is the angle between the magnetization vectors of the two electrodes. The second term G^{as} denotes impurity-assisted tunneling and is present when the barrier contains nonmagnetic impurities. The prefactor G_0^{as} is determined by the amount of dopant-induced states available to mediate the tunnel current. The *effective tunneling* polarization P_i^{as} for this process is determined by the overlap of the electrode wave functions with the unpolarized impurity states, and P_i^{as} is therefore expected to be significantly lower than for direct tunneling.¹⁵ The last term G^{ex} represents the tunnel conductance associated with spin-exchange scattering in the barrier, which as shown by Appelbaum,¹³ contains a contribution from transitions in which there is no spin flip (superscript nsf), as well as a spin-flip part (superscript sf). Here we have generalized the result of Appelbaum to a tunnel junction with magnetic electrodes, by multiplying with appropriate polarization factors. For the spin-flip part this requires a minus $\cos(\theta)$ term, since the initial and final state of the tunneling electron are of

opposite spin, with the spin recoil taken up by the magnetic scattering center. We recast the exchange term into the following more convenient form

$$G^{\text{ex}} = G_0^{\text{ex}} [1 + \alpha P_1 P_2 \cos(\theta)], \quad (5)$$

where $G_0^{\text{ex}} = G_0^{\text{nsf}} + G_0^{\text{sf}}$ and $\alpha = (G_0^{\text{nsf}} - G_0^{\text{sf}})/G_0^{\text{ex}}$ a parameter between -1 and $+1$. When $G_0^{\text{sf}} > G_0^{\text{nsf}}$, α is negative and an inverse contribution to the JMR results.

The JMR is defined¹⁹ as $(G_p - G_{\text{ap}})/G_p$, where the subscripts p and ap denote parallel ($\theta=0^\circ$) and antiparallel ($\theta=180^\circ$) electrode magnetizations, respectively. The overall JMR is determined by the relative weight of conductance due to direct, impurity-assisted and spin-exchange tunneling. A general expression is easily deduced from Eqs. (1)–(5). Two limiting cases will be considered here. In the first one, we take $G_0^{\text{ex}}=0$ and add only an impurity-assisted conductance with $P^{\text{as}}=0$ to the direct tunneling. This gives

$$\text{JMR} = \text{JMR}^0 \frac{1}{1 + R^{\text{as}} \left[1 - \left(\frac{1}{2} \right) \text{JMR}^0 \right]}, \quad (6)$$

where $R^{\text{as}} = G_0^{\text{as}}/G_0$ and JMR^0 is the JMR for the case of direct tunneling only (when $G_0^{\text{as}}, G_0^{\text{ex}}=0$). When spin-exchange scattering is present but $G_0^{\text{as}}=0$ we get

$$\text{JMR} = \text{JMR}^0 \frac{(1 + \alpha R^{\text{ex}})}{1 + R^{\text{ex}} \left[1 - \left(\frac{1 - \alpha}{2} \right) \text{JMR}^0 \right]}, \quad (7)$$

where $R^{\text{ex}} = G_0^{\text{ex}}/G_0$. The normalized magnetoresistance JMR/JMR^0 is rather *insensitive* to typical variations in JMR^0 , that might arise from differences in preparation conditions, or from the variation of T or V . Note that the strongest reduction of JMR occurs when tunneling with spin flip dominates ($\alpha = -1$).

Magnetic tunnel junctions were prepared by thermal evaporation in a high vacuum system, as described previously.^{1,18} Onto a glass substrate, with a 10 \AA Si seed layer, 80 \AA thick Co strips are deposited. Half of each individual Co strip is coated with 14 \AA of Al without dopants, for the other half a submonolayer of dopants is sandwiched between two 7 \AA thick Al layers. Liquid-nitrogen cooling of the substrate ensures a uniform dopant distribution. Subsequently, the structure is plasma oxidized in 7×10^{-2} mbar oxygen at a dc voltage of 1.8 kV , for 110 to 120 s . This completely transforms the Al *and* the dopants into oxides, as was confirmed by x-ray photoelectron spectroscopy.²⁰ Top electrodes are cross strips of $\text{Ni}_{80}\text{Fe}_{20}$ (100 – 150 \AA thick). For each individual Co bottom strip, three $\text{Ni}_{80}\text{Fe}_{20}$ cross strips go over the doped Al_2O_3 barrier and three over the clean Al_2O_3 . The latter serve as control junctions. Film thicknesses are determined with a quartz crystal monitor with an absolute accuracy of 8% .

Figure 1 displays JMR (at 77 K) as a function of the thickness t of the δ layer for Ni and Si. Data is normalized to that of the simultaneously prepared control junctions. While for Ni doping a strong reduction of JMR is observed, Si produces only a relatively weak, but nevertheless significant decrease. The difference in behavior can easily be under-

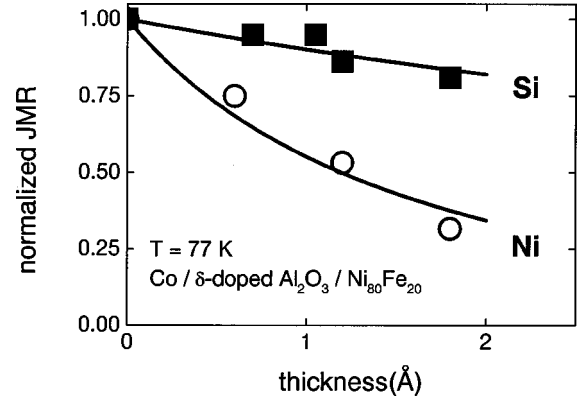


FIG. 1. Normalized JMR (at 77 K) for Co/δ -doped $\text{Al}_2\text{O}_3/\text{Ni}_{80}\text{Fe}_{20}$ tunnel junctions, as function of thickness t for Si (filled squares) and Ni (open circles). Solid lines are fits based on Eqs. (6) and (7) for Si and Ni, respectively.

stood on the basis of the expected oxidation states, i.e., Si^{2+} and/or Si^{4+} (both nonmagnetic) and Ni^{2+} and/or Ni^{3+} (both with a magnetic moment²¹ in Al_2O_3). We therefore attribute the strong effect for Ni doping to spin-exchange scattering of tunneling electrons by Ni ions, whereas the reduction found for Si is explained by assisted tunneling through Si-induced states in the barrier. This interpretation will be further corroborated by the variation with T presented below. The dopant-induced barrier states²² can be intrinsic dopant levels or arise from introduced structural disorder or defects. The solid lines in Fig. 1 represent fits based on Eq. (6) for Si and Eq. (7) for Ni, assuming R^{as} and R^{ex} proportional to t for submonolayer coverage. We obtain $R^{\text{as}}(\text{Si}) = 0.12t$ and $R^{\text{ex}}(\text{Ni}) = 0.64t$ (with t in \AA), while the value of -0.2 used for α is deduced from fits of the T dependence, to be discussed below.

Figure 2 shows resistance and JMR versus T for barriers with Si, as well as for the undoped control junction. As T is reduced from 290 to 6.5 K , the average resistance increases by a factor of 1.25 and 1.28 for the Si-doped and the control junction, respectively. Thus, the T dependence of resistance is not altered by Si doping. The behavior of JMR versus T for Si is also similar to that of the control junction, except that the JMR is reduced by an approximately temperature-independent factor (0.81 at 290 K , and 0.87 at 6.5 K). We stress that the JMR reduction is not due to the increased barrier width that results from the *addition* of Si. For, in experiments with identical tunnel junctions the JMR was found to be essentially constant for barriers formed from Al layers between 6 and 18 \AA thick.²³ Thus, increasing the barrier width by 1 or 2 \AA produces no significant change in the JMR, especially not when junctions are prepared simultaneously as done here. Hence, the observed JMR reduction is attributed to the extra conductance due to assisted tunneling via the Si-induced barrier states. The weak T dependence of the reduction indicates that this process is mainly elastic in nature. Note that the extra conductance only partially compensates for the conductance decrease due to the larger barrier width, such that the net resistance is higher with Si. Also note that for both junctions the JMR is independent of T below $\approx 40 \text{ K}$. Since the T dependence of JMR arises predominantly from thermally excited spin waves,²⁴ this sug-

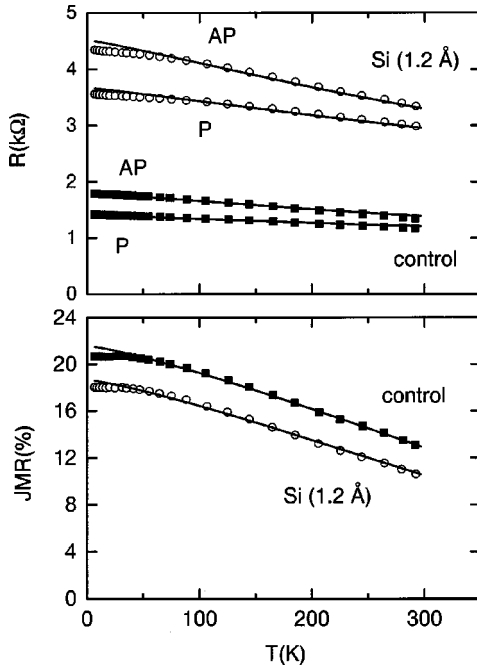


FIG. 2. Resistance (top panel) and JMR (bottom) between 6.5 and 300 K, for a junction δ doped with 1.2 Å Si (open circles), together with the corresponding undoped control junction (filled squares). Labels P and AP, respectively, denote parallel and anti-parallel magnetization of the electrodes. Solid lines are fits discussed in the text.

gests that below 40 K no spin waves are excited. This implies a low-energy cutoff of 3.5 meV in the spin-wave spectrum. A cutoff of a few meV is often observed,²⁵ and can result from anisotropy or from spatial incoherence.²⁶

Calculations^{14,17} show that impurity-assisted tunneling via a single barrier state gives an elastic, T -independent contribution to the conductance. Tunneling via two states gives a term proportional to $T^{4/3}$, due to the involvement of phonons to accommodate the energy difference between the levels.¹⁷ Our data for Si confirms the expectation¹⁵ that assisted tunneling is weakly polarized, and reduces the JMR. Assuming $P^{\text{as}}=0$ and using Eqs. (1)–(5), a good fit to both resistance and JMR versus T is obtained, see the solid lines in Fig. 2 (the cutoff in the spin-wave spectrum has not been taken into account, leading to a slight deviation between data and fits below 40 K). First the JMR and resistance versus T curves for the control junction are fitted following the procedure outlined in Ref. 24. This already includes a contribution due to spin-independent tunneling, for which several mechanisms were proposed.²⁴ Subsequently, the data for Si are fitted by only²⁷ adding to the conductance a G^{as} term, which contains a constant, and a T -dependent part with an exponent that was not fitted but taken to be $4/3$ as expected. We get for the extra spin-independent conductance due to Si-doping $R^{\text{as}} = 0.18 + 6 \times 10^{-5} T^{4/3}$ (with T in K). The first term, due to tunneling mediated by one Si level, dominates up to room T and is responsible for most of the JMR reduction. This contribution is elastic and thus persists at low T .

Results for Ni-doped barriers (Fig. 3) are quite different. A stronger T dependence of the resistance is observed, with an average resistance change by a factor of ≈ 1.9 between 290 and 6.5 K, compared to 1.35 for control junctions. Also,

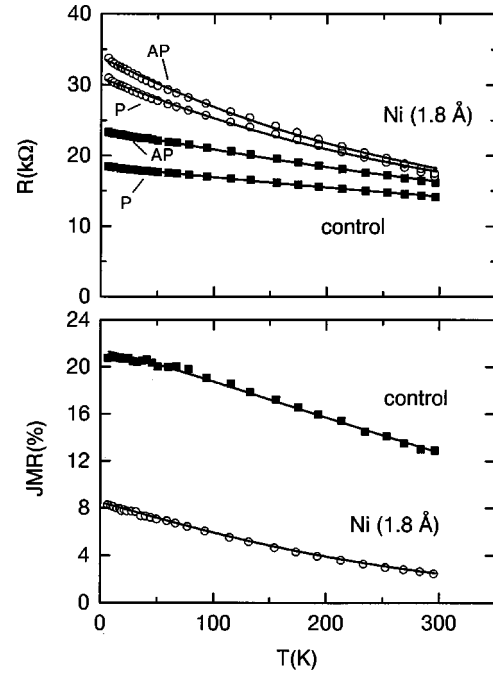


FIG. 3. Same as Fig. 2 but now for a δ layer of 1.8 Å Ni.

at low T the resistance with Ni deviates from the approximately linear behavior of the control junction. Thus, the Ni-induced conductance is (partially) frozen out upon cooling. As a result, the JMR (Fig. 3, bottom panel) goes up by more than a factor of 3, i.e., significantly faster than for the control junctions. Detailed analysis shows that fitting the JMR and resistance versus T curves simultaneously, cannot be done by adding only an unpolarized conductance (as was done for Si dopants). Rather, it requires the presence of an *inverse* con-

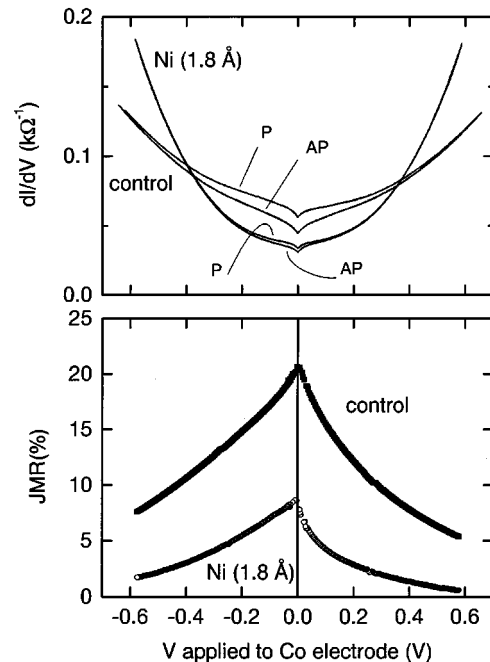


FIG. 4. Differential conductance dI/dV for parallel and anti-parallel electrode magnetizations (top panel) and JMR (bottom) versus bias voltage, for a junction δ doped with 1.8 Å Ni, together with the corresponding undoped control junction, at 6.5 K.

tribution to the JMR. The solid lines in Fig. 3 are fits, where the difference between control and Ni-doped junction is entirely²⁷ due to an added spin-exchange term $R^{\text{ex}} = 1.1 + 0.0025T^{1.1}$, with $\alpha = -0.2$. The negative α demonstrates that the process contributes inversely to the JMR, with $G_0^{\text{nsf}} > G_0^{\text{sf}}$. Note that the above values are obtained by neglecting a possible contribution from unpolarized impurity-assisted tunneling via Ni ions, and therefore represent an upper boundary of R^{ex} . If a nonzero G^{as} is included the conductance takes the form $G_0[1 + R^{\text{as}} + R^{\text{ex}} + P_1 P_2 \cos(\theta)(1 + \alpha R^{\text{ex}})]$ for $P^{\text{as}} = 0$. An equally good fit can therefore be obtained if R^{as} is nonzero for Ni. This, however, requires R^{ex} to be reduced correspondingly, which in turn requires the magnitude of α to be increased. Since $-1 \leq \alpha \leq 1$, the maximum possible $R^{\text{as}} = 4(1.1 + 0.0025T^{1.1})/5$ is obtained for $\alpha = -1$, leaving a minimum $R^{\text{ex}} = (1.1 + 0.0025T^{1.1})/5$. Thus, we cannot uniquely determine R^{as} , R^{ex} , and α , but the conclusion about the presence of a spin-exchange conductance and its inverse contribution to the JMR are left intact.

The bias voltage dependence of JMR and dI/dV for a Ni-doped junction is compared to that of the control junction in Fig. 4. With Ni in the barrier, dI/dV rises much faster with V . This implies that the ratio R^{ex} increases with V . Consequently, the JMR with Ni falls about twice as fast with V as without spin-exchange scattering. For Si, such enhanced bias dependence is not observed.

Finally, we discuss the origin of the constant and the

T -dependent contribution to R^{ex} . For a Ni layer of about 0.5 ML, we can expect that some isolated Ni ions coexist with groups of magnetically interacting Ni ions, both of which produce spin scattering. For an isolated Ni^{3+} with $S = 1/2$, spin exchange with a tunneling electron reverses the Ni^{3+} moment at the expense of the Zeeman energy $g\mu_B H_{\text{eff}}$. With H_{eff} typically < 100 Oe, the energy is equivalent to $T \approx 10$ mK. This process is thus thermally allowed over the full T range used here and is believed to be responsible for the constant spin-exchange conductance, that causes the Ni-doped barriers to have a strongly reduced JMR even at 6.5 K. To explain the T -dependent spin-scattering contribution, we propose tunneling electrons excite collective magnetic modes in groups of interacting Ni moments. The relevant temperature scale is compatible with that of our experiment.

In conclusion, we have shown that impurity scattering can drastically reduce the spin-polarization of tunneling. Non-magnetic ions reduce the JMR due to weakly or unpolarized, impurity-assisted tunneling, found to be mainly elastic. Magnetic dopants produce inelastic spin-exchange scattering which enhances the T and V dependence of JMR, and was shown to contribute inversely to the JMR with spin-flip transitions dominating.

The authors thank A. Bratkovsky, J. Nowak, and R.J.M. van de Veerdonk for stimulating and fruitful discussions. We acknowledge support from ONR, Grant No. N00014-92-J-1847 and NSF, Grant No. DMR 9423013.

-
- ¹J. S. Moodera, L. R. Kinder, T. M. Wong, and R. Meservey, Phys. Rev. Lett. **74**, 3273 (1995); J. S. Moodera and L. R. Kinder, J. Appl. Phys. **79**, 4724 (1996).
- ²T. Miyazaki and N. Tezuka, J. Magn. Magn. Mater. **139**, L231 (1995).
- ³L. F. Schelp, A. Fert, F. Fettar, P. Holody, S. F. Lee, J. L. Maurice, F. Petroff, and A. Vaurès, Phys. Rev. B **56**, R5747 (1997).
- ⁴K. Ono, H. Shimada, S. Kobayashi, and Y. Outuka, J. Phys. Soc. Jpn. **65**, 3449 (1996).
- ⁵J. Barnaś and A. Fert, Phys. Rev. Lett. **80**, 1058 (1998).
- ⁶S. Takahashi and S. Maekawa, Phys. Rev. Lett. **80**, 1758 (1998).
- ⁷S. Mitani, S. Takahashi, K. Takanashi, K. Yakushiji, S. Maekawa, and H. Fujimori, Phys. Rev. Lett. **81**, 2799 (1998).
- ⁸A. F. G. Wyatt, Phys. Rev. Lett. **13**, 401 (1964).
- ⁹J. M. Rowell and L. Y. L. Shen, Phys. Rev. Lett. **17**, 15 (1966); L. Y. L. Shen and J. M. Rowell, Phys. Rev. **165**, 566 (1968).
- ¹⁰E. L. Wolf, *Principles of Electron Tunneling Spectroscopy* (Clarendon, Oxford, 1985).
- ¹¹J. Appelbaum, Phys. Rev. Lett. **17**, 91 (1966).
- ¹²P. W. Anderson, Phys. Rev. Lett. **17**, 95 (1966).
- ¹³J. Appelbaum, Phys. Rev. **154**, 633 (1967).
- ¹⁴A. I. Larkin and K. A. Matveev, Zh. Éksp. Teor. Fiz. **93**, 1030 (1987) [Sov. Phys. JETP **66**, 580 (1987)].
- ¹⁵A. M. Bratkovsky, Phys. Rev. B **56**, 2344 (1997).
- ¹⁶R. Meservey, P. M. Tedrow, and J. S. Brooks, J. Appl. Phys. **53**, 1563 (1982); G. A. Gibson and R. Meservey, *ibid.* **58**, 1584 (1985).
- ¹⁷Y. Xu, D. Ephron, and M. R. Beasley, Phys. Rev. B **52**, 2843 (1995).
- ¹⁸R. Jansen and J. S. Moodera, J. Appl. Phys. **83**, 6682 (1998).
- ¹⁹M. Julliere, Phys. Lett. **54A**, 225 (1975).
- ²⁰R. Jansen, B. Davis, C. T. Tanaka, and J. S. Moodera (unpublished).
- ²¹S. Geschwind and J. P. Remeika, J. Appl. Phys. **33**, 370 (1962).
- ²²P. A. Cox, *Transition Metal Oxides. An Introduction to their Electronic Structure and Properties* (Clarendon, Oxford, 1992).
- ²³J. S. Moodera, E. F. Gallagher, K. Robinson, and J. Nowak, Appl. Phys. Lett. **70**, 3050 (1997). More recently, Co/Al₂O₃/CoFe junctions with Al thickness of 12.5, 14, and 15.5 Å, showed JMR of $16.9 \pm 0.8\%$, with no systematic dependence on barrier thickness.
- ²⁴C. H. Shang, J. Nowak, R. Jansen, and J. S. Moodera, Phys. Rev. B **58**, R2917 (1998).
- ²⁵R. N. Sinclair and B. N. Blockhouse, Phys. Rev. **120**, 1638 (1960).
- ²⁶From the spin-wave dispersion relation and a typical spin-wave stiffness of a few 100 meV Å², a cutoff wavelength of several nm is obtained, which is on the order of the grain size.
- ²⁷Also, the overall prefactor G_0 is adjusted to account for the increased spacing between the electrodes due to the addition of the dopants in the barrier. This only affects the absolute resistance.